

EUROPEAN ORGANIZATION FOR NUCLEAR RESEARCH

CERN-EP/98-30

25 february 1998

First Evidence for a Charm Radial Excitation, $D^{*'}$

DELPHI Collaboration

Abstract

Using D^{*+} mesons exclusively reconstructed in the DELPHI detector at LEP, an excess of $66 \pm 14(\text{stat.})$ events is observed in the $D^{*+}\pi^+\pi^-$ final state with a mass of $2637 \pm 2(\text{stat.}) \pm 6(\text{syst.}) \text{ MeV}/c^2$ and a full width smaller than $15 \text{ MeV}/c^2$ (95% C.L.). This signal is compatible with the expected decay of a radially excited $D^{*'} (J^P = 1^-)$ meson.

(Submitted to Phys. Lett. B)

P.Abreu²¹, W.Adam⁴⁹, T.Adye³⁶, P.Adzic¹¹, I.Ajinenko⁴¹, G.D.Alekseev¹⁶, R.Aleman⁴⁸, P.P.Allport²², S.Almehe²⁴, U.Amaldi⁹, S.Amato⁴⁶, P.Andersson⁴³, A.Andreazza⁹, P.Antilogus²⁵, W-D.Apel¹⁷, Y.Arnoud¹⁴, B.Äsman⁴³, J-E.Augustin²⁵, A.Augustinus⁹, P.Baillon⁹, P.Bambade¹⁹, F.Barao²¹, G.Barbiellini⁴⁵, R.Barbier²⁵, D.Y.Bardin¹⁶, G.Barker⁹, A.Baroncelli³⁹, O.Barring²⁴, M.Battaglia¹⁵, M.Baubillier²³, K-H.Becks⁵¹, M.Begalli⁶, P.Beilliere⁸, Yu.Belokopytov^{9,52}, A.C.Benvenuti⁵, C.Berat¹⁴, M.Berggren²⁵, D.Bertini²⁵, D.Bertrand², M.Besancon³⁸, F.Bianchi⁴⁴, M.Bigi⁴⁴, M.S.Bilenky¹⁶, M-A.Bizouard¹⁹, D.Bloch¹⁰, M.Bonesini²⁷, W.Bonivento²⁷, M.Boonekamp³⁸, P.S.L.Booth²², A.W.Borgland⁴, G.Borisov³⁸, C.Bosio³⁹, O.Botner⁴⁷, E.Boudinov³⁰, B.Bouquet¹⁹, C.Bourdarios¹⁹, T.J.V.Bowcock²², I.Boyko¹⁶, I.Bozovic¹¹, M.Bozzo¹³, P.Branchini³⁹, K.D.Brand³⁵, T.Brenke⁵¹, R.A.Brenner⁴⁷, R.Brown⁹, P.Bruckman³⁵, J-M.Brunet⁸, L.Bugge³², T.Buran³², T.Burgsmueller⁵¹, P.Buschmann⁵¹, S.Cabrera⁴⁸, M.Caccia²⁷, M.Calvi²⁷, A.J.Camacho Rozas⁴⁰, T.Camporesi⁹, V.Canale³⁷, M.Canepa¹³, F.Carena⁹, L.Carroll²², C.Caso¹³, M.V.Castillo Gimenez⁴⁸, A.Cattai⁹, F.R.Cavallo⁵, Ch.Cerruti¹⁰, V.Chabaud⁹, Ph.Charpentier⁹, L.Chaussard²⁵, P.Checchia³⁵, G.A.Chelkov¹⁶, M.Chen², R.Chierici⁴⁴, P.Chliapnikov⁴¹, P.Chochula⁷, V.Chorowicz²⁵, J.Chudoba²⁹, P.Collins⁹, M.Colomer⁴⁸, R.Contri¹³, E.Cortina⁴⁸, G.Cosme¹⁹, F.Cossutti³⁸, J-H.Cowell²², H.B.Crawley¹, D.Crennell³⁶, G.Crosetti¹³, J.Cuevas Maestro³³, S.Czellar¹⁵, B.Dalmagne¹⁹, G.Damgaard²⁸, M.Davenport⁹, W.Da Silva²³, A.Deghorain², G.Della Ricca⁴⁵, P.Delpierre²⁶, N.Demaria⁹, A.De Angelis⁹, W.De Boer¹⁷, S.De Brabandere², C.De Clercq², B.De Lotto⁴⁵, A.De Min³⁵, L.De Paula⁴⁶, H.Dijkstra⁹, L.Di Ciaccio³⁷, A.Di Diodato³⁷, A.Djannati⁸, J.Dolbeau⁸, K.Doroba⁵⁰, M.Dracos¹⁰, J.Drees⁵¹, K.-A.Drees⁵¹, M.Dris³¹, A.Duperrin²⁵, J-D.Durand^{25,9}, R.Ehret¹⁷, G.Eigen⁴, T.Ekelof⁴⁷, G.Ekspong⁴³, M.Ellert⁴⁷, M.Elsing⁹, J-P.Engel¹⁰, B.Erzen⁴², M.Espirito Santo²¹, E.Falk²⁴, G.Fanourakis¹¹, D.Fassouliotis¹¹, J.Fayot²³, M.Feindt¹⁷, A.Fenyuk⁴¹, P.Ferrari²⁷, A.Ferrer⁴⁸, S.Fichet²³, A.Firestone¹, P.-A.Fischer⁹, U.Flagmeyer⁵¹, H.Foeth⁹, E.Fokitis³¹, F.Fontanelli¹³, B.Franek³⁶, A.G.Frodesen⁴, R.Fruhvirth⁴⁹, F.Fulda-Quenzer¹⁹, J.Fuster⁴⁸, A.Galloni²², D.Gamba⁴⁴, M.Gandelman⁴⁶, C.Garcia⁴⁸, J.Garcia⁴⁰, C.Gaspar⁹, M.Gaspar⁴⁶, U.Gasparini³⁵, Ph.Gavillet⁹, E.N.Gaziz³¹, D.Gele¹⁰, J-P.Gerber¹⁰, L.Gerdjukov⁴¹, N.Ghodbane²⁵, I.Gil⁴⁸, F.Glege⁵¹, R.Gokieli⁵⁰, B.Golob⁴², P.Goncalves²¹, I.Gonzalez Caballero⁴⁰, G.Gopal³⁶, L.Gorn^{1,53}, M.Gorski⁵⁰, Yu.Gouz⁴¹, V.Gracco¹³, J.Grahl¹, E.Graziani³⁹, C.Green²², A.Grefrath⁵¹, P.Gris³⁸, G.Grosdidier¹⁹, K.Grzelak⁵⁰, M.Gunther⁴⁷, J.Guy³⁶, F.Hahn⁹, S.Hahn⁵¹, S.Haider⁹, A.Hallgren⁴⁷, K.Hamacher⁵¹, F.J.Harris³⁴, V.Hedberg²⁴, S.Heising¹⁷, R.Henriques²¹, J.J.Hernandez⁴⁸, P.Herquet², H.Herr⁹, T.L.Hessing³⁴, J.-M.Heuser⁵¹, E.Higon⁴⁸, S-O.Holmgren⁴³, P.J.Holt³⁴, D.Holthuizen³⁰, S.Hoorelbeke², M.Houlden²², J.Hrubic⁴⁹, K.Huet², K.Hultqvist⁴³, J.N.Jackson²², R.Jacobsson⁴³, P.Jalocha⁹, R.Janik⁷, Ch.Jarlskog²⁴, G.Jarlskog²⁴, P.Jarry³⁸, B.Jean-Marie¹⁹, E.K.Johansson⁴³, L.Jonsson²⁴, P.Jonsson²⁴, C.Joram⁹, P.Juillot¹⁰, F.Kapusta²³, K.Karafasoulis¹¹, S.Katsanevas²⁵, E.C.Katsoufis³¹, R.Keranen⁴, B.A.Khomenko¹⁶, N.N.Khovanski¹⁶, B.King²², N.J.Kjaer³⁰, O.Klapp⁵¹, H.Klein⁹, P.Kluit³⁰, D.Knoblauch¹⁷, P.Kokkinias¹¹, M.Koratzinos⁹, V.Kostioukhine⁴¹, C.Kourkoumelis³, O.Kouznetsov¹⁶, M.Krammer⁴⁹, C.Kreuter⁹, I.Kronkvist²⁴, J.Krstic¹¹, Z.Krumstein¹⁶, P.Kubinec⁷, W.Kuciewicz¹⁸, K.Kurvinen¹⁵, C.Lacasta⁹, J.W.Lamsa¹, L.Lanceri⁴⁵, D.W.Lane¹, P.Langefeld⁵¹, V.Lapin⁴¹, J-P.Laugier³⁸, R.Lauhakangas¹⁵, G.Leder⁴⁹, F.Ledroit¹⁴, V.Lefebure², L.Leinonen⁴³, A.Leisos¹¹, R.Leitner²⁹, J.Lemonne², G.Lenzen⁵¹, V.Lepeltier¹⁹, T.Lesiak¹⁸, M.Lethuillier³⁸, J.Libby³⁴, D.Liko⁹, A.Lipniacka⁴³, I.Lippi³⁵, B.Loerstad²⁴, J.G.Loken³⁴, J.H.Lopes⁴⁶, J.M.Lopez⁴⁰, D.Loukas¹¹, P.Lutz³⁸, L.Lyons³⁴, J.MacNaughton⁴⁹, J.R.Mahon⁶, A.Maio²¹, A.Malek⁵¹, T.G.M.Malmgren⁴³, V.Malychev¹⁶, F.Mandl⁴⁹, J.Marco⁴⁰, R.Marco⁴⁰, B.Marechal⁴⁶, M.Margoni³⁵, J-C.Marin⁹, C.Mariotti⁹, A.Markou¹¹, C.Martinez-Rivero³³, F.Martinez-Vidal⁴⁸, S.Marti i Garcia²², F.Matorras⁴⁰, C.Matteuzzi²⁷, G.Matthiae³⁷, F.Mazzucato³⁵, M.Mazzucato³⁵, M.Mc Cubbin²², R.Mc Kay¹, R.Mc Nulty⁹, G.Mc Pherson²², J.Medbo⁴⁷, C.Meroni²⁷, A.Miagkov⁴¹, M.Michelotto³⁵, E.Migliore⁴⁴, L.Mirabito²⁵, W.A.Mitaroff⁴⁹, U.Mjoernmark²⁴, T.Moa⁴³, R.Moeller²⁸, K.Moenig⁹, M.R.Monge¹³, X.Moreau²³, P.Morettini¹³, G.Morton³⁴, K.Muenich⁵¹, M.Mulders³⁰, L.M.Mundim⁶, W.J.Murray³⁶, B.Muryn^{14,18}, G.Myratt³⁴, T.Myklebust³², F.Naraghi¹⁴, F.L.Navarria⁵, S.Navas⁴⁸, K.Nawrocki⁵⁰, P.Negri²⁷, S.Nemecek¹², N.Neufeld⁹, W.Neumann⁵¹, N.Neumeister⁴⁹, R.Nicolaidou¹⁴, B.S.Nielsen²⁸, M.Nieuwenhuizen³⁰, V.Nikolaenko¹⁰, M.Nikolenko^{10,16}, A.Nomerotski³⁵, A.Normand²², A.Nygren²⁴, W.Oberschulte-Beckmann¹⁷, V.Obratsov⁴¹, A.G.Olshevski¹⁶, A.Onofre²¹, R.Orava¹⁵, G.Orazi¹⁰, K.Osterberg¹⁵, A.Ouraou³⁸, P.Paganini¹⁹, M.Paganoni²⁷, S.Paiano⁵, R.Pain²³, R.Paiva²¹, J.Palacios³⁴, H.Palka¹⁸, Th.D.Papadopoulou³¹, K.Papageorgiou¹¹, L.Pape⁹, C.Parkes³⁴, F.Parodi¹³, U.Parzefall²², A.Passeri³⁹, M.Pegoraro³⁵, L.Peralta²¹, H.Pernegger⁴⁹, M.Pernicka⁴⁹, A.Perrotta⁵, C.Petridou⁴⁵, A.Petrolini¹³, H.T.Phillips³⁶, G.Piana¹³, F.Pierre³⁸, M.Pimenta²¹, E.Piotto³⁵, T.Podobnik⁴², O.Podobrin⁹, M.E.Pol⁶, G.Polok¹⁸, P.Poropat⁴⁵, V.Pozdniakov¹⁶, P.Privitera³⁷, N.Pukhaeva¹⁶, A.Pullia²⁷, D.Radojicic³⁴, S.Ragazzi²⁷, H.Rahmani³¹, D.Rakoczy⁴⁹, J.Rames¹², P.N.Ratoff²⁰, A.L.Read³², P.Rebecchi⁹, N.G.Redaeli²⁷, M.Regler⁴⁹, D.Reid⁹, R.Reinhardt⁵¹, P.B.Renton³⁴, L.K.Resvanis³, F.Richard¹⁹, J.Ridky¹², G.Rinaudo⁴⁴, O.Rohne³², A.Romero⁴⁴, P.Ronchese³⁵, E.I.Rosenberg¹, P.Rosinsky⁷, P.Roudeau¹⁹, T.Rovelli⁵, V.Ruhlmann-Kleider³⁸, A.Ruiz⁴⁰, H.Saarikko¹⁵, Y.Sacquin³⁸, A.Sadovsky¹⁶, G.Sajot¹⁴, J.Salt⁴⁸, D.Sampsonidis¹¹, M.Sannino¹³, H.Schneider¹⁷, Ph.Schwemling²³, U.Schwickerath¹⁷, M.A.E.Schyns⁵¹, F.Scuri⁴⁵, P.Seager²⁰, Y.Sedykh¹⁶, A.M.Segar³⁴, R.Sekulin³⁶, R.C.Shellard⁶, A.Sheridan²², R.Silvestre³⁸, F.Simonetto³⁵, A.N.Sisakian¹⁶, T.B.Skaali³², G.Smadja²⁵, N.Smirnov⁴¹, O.Smirnova²⁴, G.R.Smith³⁶, A.Sopczak¹⁷, R.Sosnowski⁵⁰, D.Souza-Santos⁶, T.Spaso²¹, E.Spiriti³⁹, P.Sponholz⁵¹, S.Squarcia¹³, D.Stampfer⁴⁹, C.Stanescu³⁹, S.Stanic⁴², S.Stapnes³², I.Stavitski³⁵, K.Stevenson³⁴, A.Stocchi¹⁹, J.Strauss⁴⁹, R.Strub¹⁰, B.Stugu⁴, M.Szczekowski⁵⁰, M.Szeptycka⁵⁰, T.Tabarelli²⁷, F.Tegenfeldt⁴⁷, F.Terranova²⁷, J.Thomas³⁴, A.Tilquin²⁶, J.Timmermans³⁰

L.G.Tkatchev¹⁶, T.Todorov¹⁰, S.Todorova¹⁰, D.Z.Toet³⁰, A.Tomaradze², B.Tome²¹, A.Tonazzo²⁷, L.Tortora³⁹, G.Transtromer²⁴, D.Treille⁹, G.Tristram⁸, A.Trombini¹⁹, C.Troncon²⁷, A.Tsirou⁹, M-L.Turluer³⁸, I.A.Tyapkin¹⁶, S.Tzamarias¹¹, B.Ueberschaer⁵¹, O.Ullaland⁹, V.Uvarov⁴¹, G.Valenti⁵, E.Vallazza⁴⁵, G.W.Van Apeldoorn³⁰, P.Van Dam³⁰, J.Van Eldik³⁰, A.Van Lysebetten², I.Van Vulpen³⁰, N.Vassilopoulos³⁴, G.Vegni²⁷, L.Ventura³⁵, W.Venus³⁶, F.Verbeure², M.Verlato³⁵, L.S.Vertogradov¹⁶, V.Verzi³⁷, D.Vilanova³⁸, L.Vitale⁴⁵, E.Vlasov⁴¹, A.S.Vodopyanov¹⁶, V.Vrba¹², H.Wahlen⁵¹, C.Walck⁴³, C.Weiser¹⁷, A.M.Wetherell⁹, D.Wicke⁵¹, J.H.Wickens², G.R.Wilkinson⁹, M.Winter¹⁰, M.Witek¹⁸, T.Wlodek¹⁹, G.Wolf⁹, J.Yi¹, O.Yushchenko⁴¹, A.Zalewska¹⁸, P.Zalewski⁵⁰, D.Zavrtanik⁴², E.Zevgolatakos¹¹, N.I.Zimin¹⁶, G.C.Zucchelli⁴³, G.Zumerle³⁵

¹Department of Physics and Astronomy, Iowa State University, Ames IA 50011-3160, USA

²Physics Department, Univ. Instelling Antwerpen, Universiteitsplein 1, BE-2610 Wilrijk, Belgium and IIHE, ULB-VUB, Pleinlaan 2, BE-1050 Brussels, Belgium

and Faculté des Sciences, Univ. de l'Etat Mons, Av. Maistriau 19, BE-7000 Mons, Belgium

³Physics Laboratory, University of Athens, Solonos Str. 104, GR-10680 Athens, Greece

⁴Department of Physics, University of Bergen, Allégaten 55, NO-5007 Bergen, Norway

⁵Dipartimento di Fisica, Università di Bologna and INFN, Via Irnerio 46, IT-40126 Bologna, Italy

⁶Centro Brasileiro de Pesquisas Físicas, rua Xavier Sigaud 150, BR-22290 Rio de Janeiro, Brazil

and Depto. de Física, Pont. Univ. Católica, C.P. 38071 BR-22453 Rio de Janeiro, Brazil

and Inst. de Física, Univ. Estadual do Rio de Janeiro, rua São Francisco Xavier 524, Rio de Janeiro, Brazil

⁷Comenius University, Faculty of Mathematics and Physics, Mlynska Dolina, SK-84215 Bratislava, Slovakia

⁸Collège de France, Lab. de Physique Corpusculaire, IN2P3-CNRS, FR-75231 Paris Cedex 05, France

⁹CERN, CH-1211 Geneva 23, Switzerland

¹⁰Institut de Recherches Subatomiques, IN2P3 - CNRS/ULP - BP20, FR-67037 Strasbourg Cedex, France

¹¹Institute of Nuclear Physics, N.C.S.R. Demokritos, P.O. Box 60228, GR-15310 Athens, Greece

¹²FZU, Inst. of Phys. of the C.A.S. High Energy Physics Division, Na Slovance 2, CZ-180 40, Praha 8, Czech Republic

¹³Dipartimento di Fisica, Università di Genova and INFN, Via Dodecaneso 33, IT-16146 Genova, Italy

¹⁴Institut des Sciences Nucléaires, IN2P3-CNRS, Université de Grenoble 1, FR-38026 Grenoble Cedex, France

¹⁵Helsinki Institute of Physics, HIP, P.O. Box 9, FI-00014 Helsinki, Finland

¹⁶Joint Institute for Nuclear Research, Dubna, Head Post Office, P.O. Box 79, RU-101 000 Moscow, Russian Federation

¹⁷Institut für Experimentelle Kernphysik, Universität Karlsruhe, Postfach 6980, DE-76128 Karlsruhe, Germany

¹⁸Institute of Nuclear Physics and University of Mining and Metallurgy, Ul. Kawiora 26a, PL-30055 Krakow, Poland

¹⁹Université de Paris-Sud, Lab. de l'Accélérateur Linéaire, IN2P3-CNRS, Bât. 200, FR-91405 Orsay Cedex, France

²⁰School of Physics and Chemistry, University of Lancaster, Lancaster LA1 4YB, UK

²¹LIP, IST, FCUL - Av. Elias Garcia, 14-1º, PT-1000 Lisboa Codex, Portugal

²²Department of Physics, University of Liverpool, P.O. Box 147, Liverpool L69 3BX, UK

²³LPNHE, IN2P3-CNRS, Univ. Paris VI et VII, Tour 33 (RdC), 4 place Jussieu, FR-75252 Paris Cedex 05, France

²⁴Department of Physics, University of Lund, Sölvegatan 14, SE-223 63 Lund, Sweden

²⁵Université Claude Bernard de Lyon, IPNL, IN2P3-CNRS, FR-69622 Villeurbanne Cedex, France

²⁶Univ. d'Aix - Marseille II - CPP, IN2P3-CNRS, FR-13288 Marseille Cedex 09, France

²⁷Dipartimento di Fisica, Università di Milano and INFN, Via Celoria 16, IT-20133 Milan, Italy

²⁸Niels Bohr Institute, Blegdamsvej 17, DK-2100 Copenhagen Ø, Denmark

²⁹NC, Nuclear Centre of MFF, Charles University, Areal MFF, V Holesovickach 2, CZ-180 00, Praha 8, Czech Republic

³⁰NIKHEF, Postbus 41882, NL-1009 DB Amsterdam, The Netherlands

³¹National Technical University, Physics Department, Zografou Campus, GR-15773 Athens, Greece

³²Physics Department, University of Oslo, Blindern, NO-1000 Oslo 3, Norway

³³Dpto. Física, Univ. Oviedo, Avda. Calvo Sotelo s/n, ES-33007 Oviedo, Spain

³⁴Department of Physics, University of Oxford, Keble Road, Oxford OX1 3RH, UK

³⁵Dipartimento di Fisica, Università di Padova and INFN, Via Marzolo 8, IT-35131 Padua, Italy

³⁶Rutherford Appleton Laboratory, Chilton, Didcot OX11 0QX, UK

³⁷Dipartimento di Fisica, Università di Roma II and INFN, Tor Vergata, IT-00173 Rome, Italy

³⁸DAPNIA/Service de Physique des Particules, CEA-Saclay, FR-91191 Gif-sur-Yvette Cedex, France

³⁹Istituto Superiore di Sanità, Ist. Naz. di Fisica Nucl. (INFN), Viale Regina Elena 299, IT-00161 Rome, Italy

⁴⁰Instituto de Física de Cantabria (CSIC-UC), Avda. los Castros s/n, ES-39006 Santander, Spain

⁴¹Inst. for High Energy Physics, Serpukov P.O. Box 35, Protvino, (Moscow Region), Russian Federation

⁴²J. Stefan Institute, Jamova 39, SI-1000 Ljubljana, Slovenia and Department of Astroparticle Physics, School of Environmental Sciences, Kostanjevska 16a, Nova Gorica, SI-5000 Slovenia,

and Department of Physics, University of Ljubljana, SI-1000 Ljubljana, Slovenia

⁴³Fysikum, Stockholm University, Box 6730, SE-113 85 Stockholm, Sweden

⁴⁴Dipartimento di Fisica Sperimentale, Università di Torino and INFN, Via P. Giuria 1, IT-10125 Turin, Italy

⁴⁵Dipartimento di Fisica, Università di Trieste and INFN, Via A. Valerio 2, IT-34127 Trieste, Italy

and Istituto di Fisica, Università di Udine, IT-33100 Udine, Italy

⁴⁶Univ. Federal do Rio de Janeiro, C.P. 68528 Cidade Univ., Ilha do Fundão BR-21945-970 Rio de Janeiro, Brazil

⁴⁷Department of Radiation Sciences, University of Uppsala, P.O. Box 535, SE-751 21 Uppsala, Sweden

⁴⁸IFIC, Valencia-CSIC, and D.F.A.M.N., U. de Valencia, Avda. Dr. Moliner 50, ES-46100 Burjassot (Valencia), Spain

⁴⁹Institut für Hochenergiephysik, Österr. Akad. d. Wissensch., Nikolsdorfergasse 18, AT-1050 Vienna, Austria

⁵⁰Inst. Nuclear Studies and University of Warsaw, Ul. Hoza 69, PL-00681 Warsaw, Poland

⁵¹Fachbereich Physik, University of Wuppertal, Postfach 100 127, DE-42097 Wuppertal, Germany

⁵²On leave of absence from IHEP Serpukhov

⁵³Now at University of Florida

1 Introduction

In the spectroscopy of charm mesons, the D and D^{*} ground states are well established while only the narrow orbital excitations D₁ and D₂^{*} have been clearly observed so far [1]. For mesons containing heavy and light quarks (Q \bar{q}) and in the limit where the heavy quark mass is much larger than the typical QCD scale ($m_Q \gg \Lambda_{\text{QCD}}$), the spin \vec{s}_Q of the heavy quark and the total (spin+orbital) angular momentum $\vec{j}_q = \vec{s}_q + \vec{L}$ of the light component are separately conserved by the strong interaction [2]. This heavy quark symmetry, together with quark potential models used for lower mass mesons, allows the masses and decay widths of heavy mesons of total spin $\vec{J} = \vec{s}_Q + \vec{j}_q$ to be predicted [3–7]. The D and D^{*} correspond to the two degenerate levels of the ($L = 0, j_q = 1/2$) state. The $L = 1$ orbital excitations are grouped into two degenerate levels with $j_q = 1/2$ and $j_q = 3/2$. The $j_q = 1/2$ states decay through an S-wave and are expected to have a large decay width, whereas the $j_q = 3/2$ states decay through a D-wave and are narrow. This scheme is summarized in table 1 for non-strange charmed mesons. The D₁(2420) and D₂^{*}(2460) have been observed with decay widths of about 20 MeV/ c^2 and are identified as the states with $j_q = 3/2$ and $J^P = 1^+$ and 2^+ , respectively [1]. Orbitally excited beauty mesons are expected to present a similar scheme.

	$J^P j_q$		Mass (MeV/ c^2)	, Width (MeV/ c^2)	Decay modes
D ₀ [*]	0 ⁺ 1/2		~ 2360	≥ 170	(D π)
D ₁ ⁺	1 ⁺ 1/2		~ 2430	≥ 250	(D [*] π)
D ₁	1 ⁺ 3/2	D ₁ ⁺	2427 ± 5	28 ± 8	D ^{*0} π^+ (D ^{*+} π^0 , D ρ , D $\pi\pi$)
		D ₁ ⁰	2422.2 ± 1.8	$18.9_{-3.5}^{+4.6}$	D ^{*+} π^- (D ^{*0} π^0 , D ρ , D $\pi\pi$)
D ₂ [*]	2 ⁺ 3/2	D ₂ ^{*+}	2459 ± 4	25_{-7}^{+8}	D ⁰ π^+ , D ^{*0} π^+ (D ^{(*)+} π^0 , D [*] ρ , D [*] $\pi\pi$)
		D ₂ ^{*0}	2458.9 ± 2.0	23 ± 5	D ⁺ π^- , D ^{*+} π^- (D ^{(*)0} π^0 , D [*] ρ , D [*] $\pi\pi$)

Table 1: Expected and observed $L = 1$ orbital excitations of D⁰ and D⁺ mesons. The broad $j_q = 1/2$ states are estimated according to [7]. The narrow $j_q = 3/2$ states are measured [1]. In the last column, those predicted decay modes which are not yet observed are indicated within parentheses.

In addition to these orbital excitations, radial excitations of heavy mesons are also foreseen. Based on a QCD inspired relativistic quark model, the D['] ($J^P = 0^-$) and D^{*'} ($J^P = 1^-$) are expected with masses of 2.58 GeV/ c^2 and 2.64 GeV/ c^2 , respectively, with a 10-25 MeV/ c^2 uncertainty on the mass predictions [4]. A recent relativistic quark model, which requires no expansion in function of the lightest quark mass, predicts masses of 2.58 GeV/ c^2 and 2.63 GeV/ c^2 , respectively, with an agreement of better than 20 MeV/ c^2 for the observed charm orbital states [8]. The dominant decay modes of the D['] and D^{*'} are expected to be into D $\pi\pi$ and D^{*} $\pi\pi$, respectively, but decays into D^(*) ρ or through an intermediate orbital excitation are not excluded. Decays with a single pion in the final state would require a P-wave transition and should be suppressed. However no firm estimate of the decay widths is available. The decay amplitudes of known light quark mesons are reasonably well described using harmonic oscillator wave functions for the initial and final state mesons [6]. Using this approach for charm mesons provides an

estimate of the $D^{*'}$ partial decay widths of less than one MeV/c^2 in the $D^*\pi\pi$ final state and less than a few MeV/c^2 in the $D_1^{(')}\pi$ final state. Figure 1 shows the spectrum of the various D mesons with their decay modes involving S-, P- or D-wave transitions. In the B sector, a narrow resonance compatible with the expectation of a $B^{(*)'}$ decaying into $B^{(*)}\pi^+\pi^-$ has been reported [9].

This letter presents evidence for a narrow $D^{*+}\pi^+\pi^-$ resonance ¹ using about 3 million Z decays observed in DELPHI from 1992 to 1995. The D^{*+} candidates are selected in the exclusive decay channels $D^{*+} \rightarrow D^0\pi^+$ followed by $D^0 \rightarrow K^-\pi^+$ or $D^0 \rightarrow K^-\pi^+\pi^+\pi^-$. Then the known D_1^0 and D_2^{*0} decaying into $D^{*+}\pi^-$ are used in order to check the vertex finding procedure and the invariant mass estimate. Finally, $D^{*+}\pi^+\pi^-$ final states are considered.

2 The DELPHI detector

The DELPHI detector and its performance have been described in detail elsewhere [10,11]; only those components relevant for the present analysis are discussed here.

The tracking of charged particles is accomplished in the barrel region with a set of cylindrical tracking detectors whose axes are oriented along the 1.23 T magnetic field and the direction of the beam.

The Time Projection Chamber (TPC), the main tracking device, is a cylinder of 30 cm inner radius, 122 cm outer radius and length 2.7 m. For polar angles between 39° and 141° it provides up to 16 space points along the charged particle trajectory.

The Vertex Detector (VD), located nearest to the LEP interaction region, has an intrinsic $R\phi$ resolution of 5–6 μm , transverse to the beam direction, and consists of three concentric layers of silicon microstrip detectors at average radii of 6.3 cm, 9.0 cm, and 10.9 cm. The layers surround the beam pipe, a beryllium cylinder of inner radius 5.3 cm and wall thickness 1.45 mm. In the earlier runs all the VD layers were single-sided with strips parallel to the beam axis. In 1994 and 1995 the innermost and the outermost layers were replaced by double-sided silicon microstrip modules, allowing measurements to be made parallel to the beam.

The VD, the Inner Detector (ID), the TPC and the Outer Detector (OD), measure the charged particle tracks at polar angles, θ , between 30° and 150° . Combining the information from these detectors, a resolution, $\sigma(p)/p$, of $\pm 3.0\%$ has been obtained for muons of 45 GeV/c momentum.

Hadrons are identified using the specific ionization (dE/dx) in the TPC and the Cherenkov radiation in the barrel Ring Imaging Cherenkov detector (RICH) placed between the TPC and the OD detectors.

The tracking in the forward ($11^\circ < \theta < 33^\circ$) and backward ($147^\circ < \theta < 169^\circ$) regions is improved by two pairs of Forward drift Chambers (FCA and FCB) in the end-caps.

3 The event sample and the simulation

Charged particles were selected as follows: the momentum had to be between 0.1 GeV/c and 50 GeV/c , the relative error on momentum measurement less than 100%, the track length in the TPC had to be larger than 30 cm, the projection of their impact parameter relative to the interaction point had to be below 4 cm in the plane transverse

¹Throughout the paper charge-conjugate states are implicitly included and the pion from the D^{*+} decay is denoted π^+_{*} .

to the beam direction and the distance to the interaction point along the beam direction below 10 cm.

Hadronic events were selected by requiring five or more charged particles (of momentum larger than 0.4 GeV/ c) and a total energy of charged particles larger than 12% of the collision energy, assuming all charged particles to be pions. A total of 3.4 million hadronic events was obtained from the 1992-1995 data at centre-of-mass energies close to the Z mass.

Simulated hadronic events were generated with the JETSET 7.3 Parton Shower program [12]. The generated events were followed through a detailed detector simulation [11] which included simulation of secondary interactions and digitization of all electronic signals. The simulated data were then processed through the same analysis chain as the real data.

In order to estimate the reconstruction efficiencies and the invariant mass resolutions, some dedicated samples of events containing a D_1^0 or D_2^{*0} decaying into $D^{*+}\pi^-$, or a $D^{*'} decaying into $D^{*+}\pi^+\pi^-$, were generated. Both modes $D^{*+} \rightarrow D^0\pi^+$ with $D^0 \rightarrow K^-\pi^+$ or $D^0 \rightarrow K^-\pi^+\pi^+\pi^-$ were simulated. The $D^{*'} mass was arbitrarily fixed to 2640 MeV/ c^2 .$$

4 D^{*+} meson reconstruction

The primary interaction vertex was computed in space for each event using an iterative procedure based on the χ^2 of the fit of all charged particle trajectories [11]. The average transverse position of the interaction point, measured for each fill, was included as a constraint during the primary vertex fit.

For the D^0 from D^{*+} decay, all $K^-\pi^+$ and $K^-\pi^+\pi^+\pi^-$ combinations were tried to fit a secondary vertex in space. The D^0 momentum was taken as the sum of the momenta of the decay products from this secondary vertex. Kaon candidates were considered if they had a momentum larger than 1 GeV/ c . Pion candidates were considered if they had a momentum larger than 1 GeV/ c in the $K\pi$ channel and 0.5 GeV/ c in the $K3\pi$ channel. At least two particle tracks from the D^0 decay were required to have at least one hit in the VD. A distance ΔL was computed between the primary and secondary vertices in the plane transverse to the beam axis. This distance was given the same sign as the scalar product of the D^0 momentum with the vector joining the primary to the secondary vertices.

The D^0 apparent proper time $t(D^0)$ was defined as $t(D^0) = \Delta L \cdot M(D^0)/p_t(D^0)$ where $M(D^0)$ is the reconstructed mass of the D^0 and $p_t(D^0)$ is its transverse momentum relative to the beam axis.

To reduce the combinatorial background in the $K\pi$ channel where no K identification was applied, the angle θ^* between the D^0 flight direction and the kaon direction in the D^0 rest frame was required to satisfy the condition $\cos \theta^* > -0.9$. For genuine D^0 candidates an isotropic distribution in $\cos \theta^*$ is expected whereas the background is strongly peaked in the backward direction.

In the $K3\pi$ channel further selections were required to reduce the combinatorial background: an impact parameter, computed in the plane transverse to the beam direction, of each charged particle track relative to their common D^0 vertex smaller than 300 μm , a χ^2 probability of the D^0 vertex larger than 1%, a kaon candidate compatible with the expectation according to the combined RICH and dE/dx identification and a positive distance ΔL .

Then all charged particles with momentum between 0.4 GeV/ c and 4.5 GeV/ c and charge opposite to that of the kaon candidate of the D^0 were used as pion candidates

for the $D^{*+} \rightarrow D^0 \pi^+$ decay. The D^{*+} candidates were selected if their energy fraction $X_E(D^{*+}) = E(D^{*+})/E_{\text{beam}}$ was larger than 0.25.

In the $K\pi$ ($K3\pi$) channel, events were selected if the mass difference $M(K\pi\pi_*) - M(K\pi)$ ($M(K3\pi\pi_*) - M(K3\pi)$) was within ± 2 (± 1) MeV/c^2 of the nominal ($D^{*+} - D^0$) mass difference.

The invariant mass distributions $M(K^-\pi^+)$ and $M(K^-\pi^+\pi^+\pi^-)$ are shown in figure 2. They were each fitted by using the following contributions: the exponential of a second order polynomial function for the combinatorial background and the sum of two Gaussian functions (of common mean) for the D^0 candidates. A parameterization of the $D^0 \rightarrow K^-\pi^+\pi^0$ reflection (with free normalization) was also included in the fit of the $K^-\pi^+$ invariant mass distribution. The fitted D^0 mass is 1868 ± 1 (1869 ± 1) MeV/c^2 and the observed r.m.s. width of the narrower Gaussian is 19 ± 1 (12 ± 1) MeV/c^2 in the $K\pi$ ($K3\pi$) channel. In both decay modes, the measured D^0 mass was found about 4 MeV/c^2 above the expectation of $1864.5 \pm 0.5 \text{ MeV}/c^2$ [1]. This deviation has a negligible contribution to the systematic error described later.

In the following, for the $K\pi$ (or $K3\pi$) channel, the mass difference will be required to lie within ± 2 (± 1) MeV/c^2 of the nominal ($D^{*+} - D^0$) mass difference and the reconstructed D^0 invariant mass to lie within ± 40 (± 30) MeV/c^2 of the nominal D^0 mass. These selections provided $4661 \pm 88(\text{stat.})$ and $2164 \pm 65(\text{stat.})$ reconstructed D^{*+} in the respective channels.

5 Search for orbitally excited D mesons

In this section a search for orbitally excited D_1^0 and D_2^{*0} mesons decaying into $D^{*+}\pi^-$ is presented. Using the pion from the $D^{*+} \rightarrow D^0 \pi^+$ decay, a $D^0 \pi^+ \pi^-$ vertex can be fitted. In the next section a similar vertex fit is applied to the search for $D^{*+}\pi^+\pi^-$ final states. The study of the well known D_1^0 and D_2^{*0} mesons can thus be used as a test of the method.

In the $D^{*+}\pi^-$ final state, all pion candidates of charge opposite to the D^{*+} and momentum greater than 1.0 (1.5) GeV/c were considered in the $K\pi$ ($K3\pi$) channel. Then, the pion from $D^{*+} \rightarrow D^0 \pi^+$ decay was used to fit a $D^0 \pi^+ \pi^-$ vertex. At least one pion had to be detected in the VD. In the $D^0 \rightarrow K^-\pi^+$ channel, the additional π^- was selected if its impact parameter with respect to the common $D^0 \pi^+ \pi^-$ vertex was less than 50 μm . This requirement was not used in the $K3\pi$ channel due to the better definition of D^0 decay vertex in this case.

To estimate the $M(D^{*+}\pi^-)$ invariant mass, the mass difference $M(D^{*+}\pi^-) = M(D^0 \pi^+ \pi^-) - M(D^0 \pi^+) + m_{D^*}$ was computed, where m_{D^*} is the nominal D^{*+} mass [1]. According to the simulation, this gives a resolution of about 6 MeV/c^2 on $M(D^{*+}\pi^-)$ with no bias in the mass computation.

This invariant mass distribution is presented in figure 3 for the selected events. An excess of ($D^{*+}\pi^-$) pairs is observed between 2.4 and 2.5 GeV/c^2 , but not in the ($D^{*+}\pi^+$) sample. The $M(D^{*+}\pi^-)$ distribution was fitted as the sum of three contributions: a function of the form $\alpha(M(D^*\pi) - m_{D^*} - m_\pi)^\beta \cdot \exp(-\gamma(M(D^*\pi) - m_{D^*} - m_\pi))$ for the background, where m_π is the pion mass, and two functions describing both D_1^0 and D_2^{*0} resonances. Each resonance shape was parameterized as the convolution of a Breit-Wigner and a Gaussian function of same mean value. The full width of each Breit-Wigner function was fixed to its world average value [1] (see table 1) and the width of the Gaussian shape was set to the estimated mass resolution of 6 MeV/c^2 . The overall number and relative proportions of the resonant states and their average masses were left free in the fit. A total number of 361 ± 58 D_1^0 and D_2^{*0} was observed of which $(65 \pm 10)\%$ was assigned to the

D_1^0 meson. The fitted masses were $2425 \pm 3 \text{ MeV}/c^2$ for the D_1^0 and $2461 \pm 6 \text{ MeV}/c^2$ for the D_2^{*0} resonances, in agreement with their world average values of $2422 \pm 2 \text{ MeV}/c^2$ and $2459 \pm 2 \text{ MeV}/c^2$, respectively [1]. All fitted errors are statistical only.

6 Search for a radially excited D meson

Repeating a similar procedure as above, all remaining opposite charge $\pi^+\pi^-$ pairs produced in the same direction as the D^{*+} candidates were used to fit a $D^0\pi^+\pi^-$ vertex. In the $K\pi$ ($K3\pi$) channel, the additional pions were required to have a momentum larger than 0.6 (1.0) GeV/c . Those pion candidates compatible with a kaon according to the combined RICH and dE/dx identification were rejected. The energy fraction $X'_E(D^{*+}\pi^+\pi^-)$ and the decay length $\Delta L'$ (with an uncertainty $\sigma_{L'}$) of the $D^0\pi^+\pi^-$ vertex were computed. In order to reduce further the combinatorial background, only events belonging to $b\bar{b}$ or $c\bar{c}$ enriched samples were retained. In the $b\bar{b}$ sample the probability, P_E [11,13], that all charged particles originate from the primary vertex was required to be smaller than 0.01 and the decay length significance $\Delta L'/\sigma_{L'}$ had to be larger than 2. If these selections were not fulfilled, the D^0 apparent proper time, defined in section 4, was required to be larger than 1 ps. In the $c\bar{c}$ sample, a significance $|\Delta L'/\sigma_{L'}|$ less than 2, a D^0 apparent proper time less than 1 ps, and either a P_E value larger than 0.1 or an energy fraction X'_E greater than 0.4 were required. According to the simulation, the fraction of genuine $b\bar{b}$ ($c\bar{c}$) events was $84 \pm 2\%$ ($87 \pm 2\%$) in the enriched samples.

The reconstructed invariant mass was computed with a procedure similar to that described in section 5: $M(D^{*+}\pi^+\pi^-) = M(D^0\pi^+\pi^-) - M(D^0\pi^+) + m_{D^*}$. This gives a resolution of about $6 \text{ MeV}/c^2$ and no bias, according to the simulation. The invariant mass distribution of all $D^{*+}\pi^+\pi^-$ candidates is presented in figure 4. A narrow peak is observed whereas the wrong charge combinations $D^{*+}\pi^-\pi^-$ do not show any excess. A binned maximum likelihood fit to the mass distribution was performed by taking into account two contributions: a function of the form $\alpha(M(D^*\pi\pi) - m_{D^*} - \mu)^\beta \cdot \exp(-\gamma(M(D^*\pi\pi) - m_{D^*} - \mu))$ for the background, with μ set to $340 \text{ MeV}/c^2$, and a Gaussian function with free parameters to describe the narrow peak. The χ^2 per degree of freedom was 60/59 (it would be 91/62 if the fit was performed with the background shape only, without the Gaussian function). The fitted number of events was 66 ± 14 with a significance of 4.7 standard deviations. The fitted width was $7 \pm 2 \text{ MeV}/c^2$, in agreement with the expected resolution, and the average mass was found to be $2637 \pm 2 \text{ MeV}/c^2$. About $(57 \pm 10)\%$ of these events were selected in the $c\bar{c}$ enriched sample. Only statistical errors are quoted.

A Breit-Wigner convoluted with a Gaussian function of same mean value was also used to fit the signal shape. Fixing the width of the Gaussian to the estimated resolution of $6 \text{ MeV}/c^2$ and letting free the full width of the Breit-Wigner did not change the fitted mass value, but the fitted full width, $4.4^{+6.4}_{-4.4} \text{ MeV}/c^2$, was compatible with zero. A 95% C.L. upper limit of $15 \text{ MeV}/c^2$ is derived for the full decay width of the resonance.

The observed signal is likely to come from a $D^{*'}$ radial excitation (2^3S_1) with an expected mass of about $2630 - 2640 \text{ MeV}/c^2$ [4,8] and a full width which could be of a few MeV/c^2 [6].

Due to the momentum selections applied to the $\pi^+\pi^-$ candidates, the number of entries in the $M(D^{*+}\pi^+\pi^-)$ distribution at low mass values is slightly depleted. In the background parameterization, changing the value of the μ parameter between $280 \text{ MeV}/c^2$ and $360 \text{ MeV}/c^2$ varied the number of fitted events by ± 1 , without affecting the fitted mass and width. Changing the selection cuts did not vary the fitted mass by more than its statistical error. The effect of the $4 \text{ MeV}/c^2$ discrepancy in the measured D^0 mass was

found to be less than one MeV/c^2 on the $D^{*'}$ mass because the latter was computed as a mass difference where the measured D^0 mass cancels. A systematic uncertainty of $\pm 6 \text{ MeV}/c^2$ on the $D^{*'}$ mass can be conservatively inferred from the statistical precision on the D_1^0 and D_2^{*0} fitted masses in section 5.

No signal was found for the decay $D_2^{*+}(2459) \rightarrow D^{*+}\pi^+\pi^-$ which is kinematically disfavoured [3] and which was also reduced by the selection cuts.

As a cross-check of the assignment of a radial excitation to the observed signal, the $(\pi^+\pi^-)$ invariant mass distribution was compared to the universal form of ref. [14], assuming the $D^{*'}$ to decay directly into $D^*\pi\pi$. However the available statistics did not allow this prediction to be distinguished from the simple phase space contribution.

Finally, the production fraction of $D^{*'}$ was compared to D_1^0 and D_2^{*0} . According to the simulation, $D^{*'}$ candidates had an overall reconstruction and selection efficiency of about 4% (2%) in the $K\pi$ ($K3\pi$) decay mode of the D^0 , respectively. The corresponding efficiencies were about 14% (6%) for the observed orbital resonances. From these values and the fitted numbers of D excited states, the relative yield of $D^{*'}$ was inferred:

$$\frac{\langle N_{D^{*'+}} \rangle Br(D^{*'+} \rightarrow D^{*+}\pi^+\pi^-)}{\sum_{J=1,2} \langle N_{D^{(*)0}} \rangle Br(D_J^{(*)0} \rightarrow D^{*+}\pi^-)} = 0.49 \pm 0.18(\text{stat.}) \pm 0.10(\text{syst.}). \quad (1)$$

As most of the selection criteria of the orbital and radial transitions are similar, their uncertainties cancel in the ratio. The remaining systematics include the statistical error on the simulated samples, the error on the full width of the orbital resonances [1] and the estimate of the kaon rejection efficiency which is applied in the $D^{*+}\pi^+\pi^-$ final state. The uncertainty due to the momentum selection of the final state pions, which may depend on the different decay channels of the $D^{*'}$ (see figure 1), is not taken into account.

The result (1) can be compared with models of primary hadron production. In the thermodynamical approach of ref. [15], particles are assumed to be produced in a hadron gas at thermal and chemical equilibrium with a temperature $T = 160.3 \pm 3.7 \text{ MeV}/c^2$. In the semi-empirical approach of ref. [16], quark pair creation in a colour string field is assumed to follow a tunnelling process with an effective temperature $T' = 298 \pm 15 \text{ MeV}/c^2$. In these models, the prediction for the multiplicity of non-strange charm mesons in $c\bar{c}$ events depends only on their mass and total spin:

$$\langle N_D \rangle \propto (2J+1) K_2(m_D/T) [15] \quad (2)$$

$$\langle N_D \rangle \propto (2J+1) e^{-m_D/T'} [16], \quad (3)$$

where K_2 is the McDonald function of order 2 and formula (2) can be approximated as $(2J+1) m_D^{1.5} e^{-m_D/T}$ in the limit where $m_D \gg T$. The relative proportions of primary charm mesons $D_1:D_2^{*}:D^{*'}$ will be thus 1:1.35:0.29 [15] and 1:1.47:0.49 [16], respectively. The D_2^* can decay both into $D\pi$ and $D^*\pi$ with the measured partial width ratio, $(D_2^{*0} \rightarrow D^+\pi^-)/(D_2^{*0} \rightarrow D^{*+}\pi^-) = 2.3 \pm 0.6$ [1] whereas spin-parity conservation prevents the D_1 to decay into $D\pi$. From isospin conservation, neglecting decays into $D^{(*)}\pi\pi$ or $D^{(*)}\rho$, the following branching fraction can be estimated: $Br(D_1^0 \rightarrow D^{*+}\pi^-) = 2/3$ and $Br(D_2^{*0} \rightarrow D^{*+}\pi^-) = 0.20 \pm 0.04$. If the $D^{*'}$ decays mainly into $D^*\pi\pi$, neglecting decays into $D_1^{(*)}\pi$ or $D_2^*\pi$, isospin conservation infers $Br(D^{*'+} \rightarrow D^{*+}\pi^+\pi^-) = 1/2$. The relative yield given in eq. (1) is thus predicted to be 0.16 ± 0.01 [15] or 0.25 ± 0.02 [16] for $c\bar{c}$ events. The measured value in Z decays, where both $c\bar{c}$ and $b\bar{b}$ events contribute, is larger than these expectations but has a large uncertainty.

7 Conclusion

Using about 7000 exclusively reconstructed $D^{*\pm}$ mesons, a search for $D^{*+}\pi^+\pi^-$ decay vertices has been performed. A narrow peak is observed in the invariant mass distribution, whose width is compatible with the detector resolution. A signal of $66 \pm 14(\text{stat.})$ events is obtained with an observed mass of $2637 \pm 2(\text{stat.}) \pm 6(\text{syst.}) \text{ MeV}/c^2$ and a 95% C.L. upper limit on the full decay width of $15 \text{ MeV}/c^2$. The relative yield of these candidates corresponds to 0.49 ± 0.21 of the production fraction of orbitally excited $D_J^{(*)0}$ decaying into $D^{*+}\pi^-$. This signal is interpreted as the first evidence for a radially excited D^* ($J^P = 1^-$) meson, as predicted in refs. [4,8].

Acknowledgements

We are greatly indebted to our technical collaborators and to the funding agencies for their support in building and operating the DELPHI detector, and to the members of the CERN-SL Division for the excellent performance of the LEP collider.

We are also grateful to the technical and engineering staffs in our laboratories and we acknowledge the support of

Austrian Federal Ministry of Science, Research and Arts,

FNRS-FWO, Belgium,

FINEP, CNPq, CAPES, FUJB and FAPERJ, Brazil,

Czech Ministry of Industry and Trade, GA CR 202/96/0450 and GA AVCR A1010521,

Danish Natural Research Council,

Commission of the European Communities (DG XII),

Direction des Sciences de la Matière, CEA, France,

Bundesministerium für Bildung, Wissenschaft, Forschung und Technologie, Germany,

General Secretariat for Research and Technology, Greece,

National Science Foundation (NSF) and Foundation for Research on Matter (FOM),

The Netherlands,

Norwegian Research Council,

State Committee for Scientific Research, Poland, 2P03B00108, 2P03B03311 and 628/E-78-SPUB-P03-023/97,

JNICT-Junta Nacional de Investigação Científica e Tecnológica, Portugal,

Vedecka grantova agentura MS SR, Slovakia, Nr. 95/5195/134,

Ministry of Science and Technology of the Republic of Slovenia,

CICYT, Spain, AEN96-1661 and AEN96-1681,

The Swedish Natural Science Research Council,

Particle Physics and Astronomy Research Council, UK,

Department of Energy, USA, DE-FG02-94ER40817.

References

- [1] Particle Data Group, “Review of Particle Properties”, Phys. Rev. **D54** (1996) 1.
- [2] N. Isgur and M.B. Wise, Phys. Rev. Lett. **66** (1991) 1130 and ref. therein.
- [3] E.J. Eichten, C.T. Hill and C. Quigg, Phys. Rev. Lett. **71** (1993) 4116 and update FERMILAB-CONF-94/118-T;
Fayyazuddin and Riazuddin, Phys. Rev. **D48** (1993) 2224 and Phys. Rev. **D49** (1994) 3385;
A.F. Falk and T. Mehen, Phys. Rev. **D53** (1996) 231.
- [4] S. Godfrey and N. Isgur, Phys. Rev. **D32** (1985) 189.
- [5] J. Rosner, Comments on Nucl. and. Part. Phys. **16** (1986) 109 and ref. therein;
A.B. Kaidalov, and A.V. Nogteva, Sov. J. Nucl. Phys. **47** (1988) 321.
- [6] R. Kokoski and N. Isgur, Phys. Rev. **D35** (1987) 907.
- [7] S. Godfrey and R. Kokoski, Phys. Rev. **D43** (1991) 1679.
- [8] D. Ebert, R.N. Faustov and V.O. Galkin, “Mass spectrum of orbitally and radially excited heavy-light mesons in the relativistic quark model”, preprint HUB-EP-97/90, hep-ph/9712318 (1997).
- [9] DELPHI collab., M. Feindt and O. Podobrin, “First Observation of Radially Excited B Mesons”, contribution to ICHEP’96, ref. pa01-021, DELPHI 96-93 CONF 22 (June 1996).
- [10] DELPHI collab., P. Aarnio et al., Nucl. Instr. & Meth. **A303** (1991) 233.
- [11] DELPHI collab., P. Abreu et al., Nucl. Instr. & Meth. **A378** (1996) 57.
- [12] T. Sjöstrand, Comp. Phys. Comm. **39** (1986) 347;
T. Sjöstrand and M. Bengtsson, Comp. Phys. Comm. **43** (1987) 367;
T. Sjöstrand, JETSET 7.3 manual, CERN-TH 6488/92 (1992).
- [13] G. Borisov and C. Mariotti, Nucl. Instr. & Meth. **A372** (1996) 181.
- [14] L.S. Brown and R.N. Cahn, Phys. Rev. Lett. **35** (1975) 1;
E.J. Eichten and C. Quigg, Phys. Rev. **D49** (1994) 5845.
- [15] F. Becattini, Zeit. Phys. **C69** (1996) 485; Zeit. Phys. **C76** (1997) 269; J. Phys. **G23** (1997) 1933.
- [16] Yi-Jin Pei, Zeit. Phys. **C72** (1996) 39; see also P.V. Chliapnikov and V.A. Uvarov, Phys. Lett. **B 345** (1995) 313.

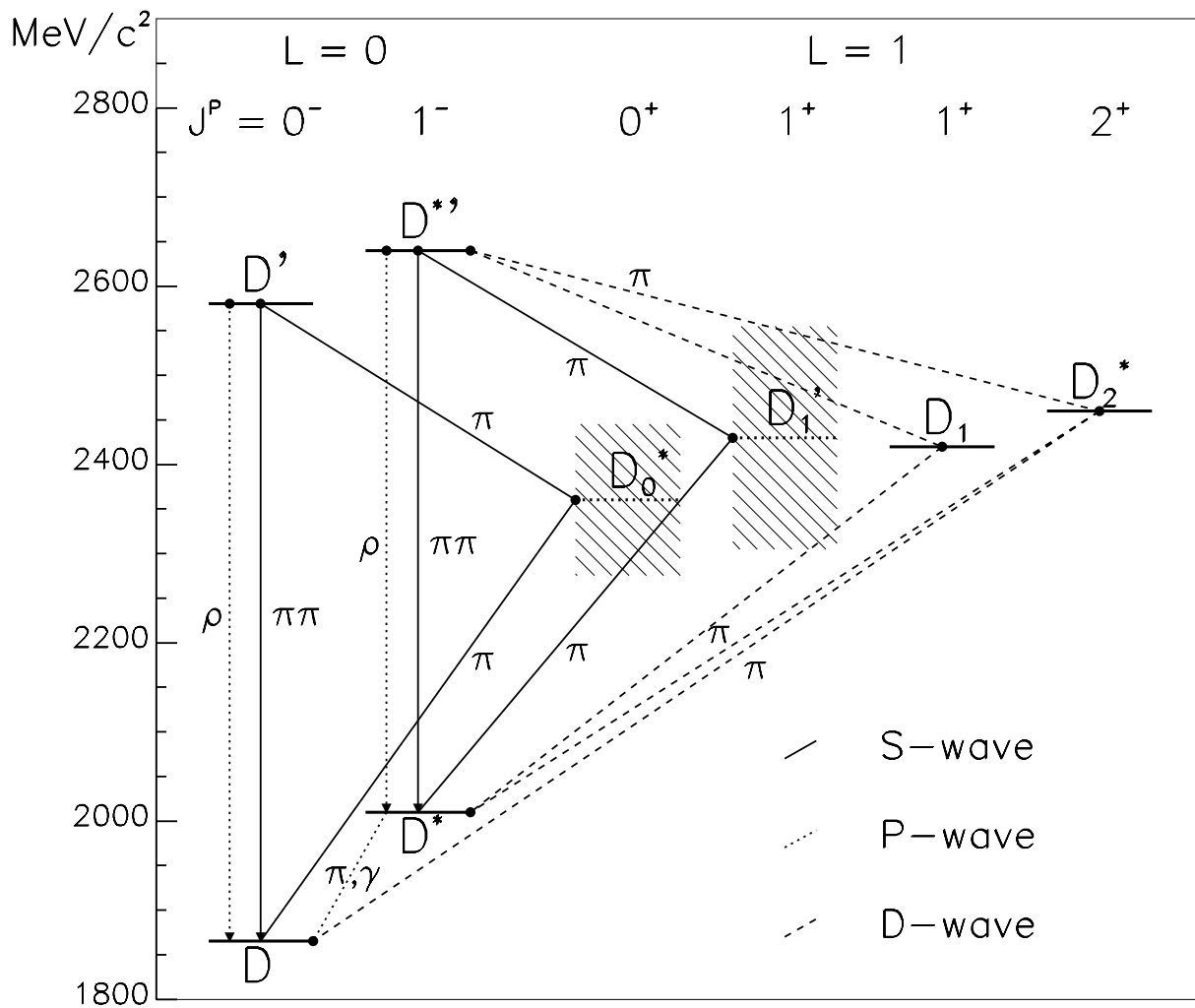


Figure 1: Spectroscopy of non-strange D mesons. The shaded areas show predicted widths for these states. For clarity the expected D_1 and D_2^* decays involving a ρ meson or $\pi\pi$ pair are not shown (see also table 1).

DELPHI

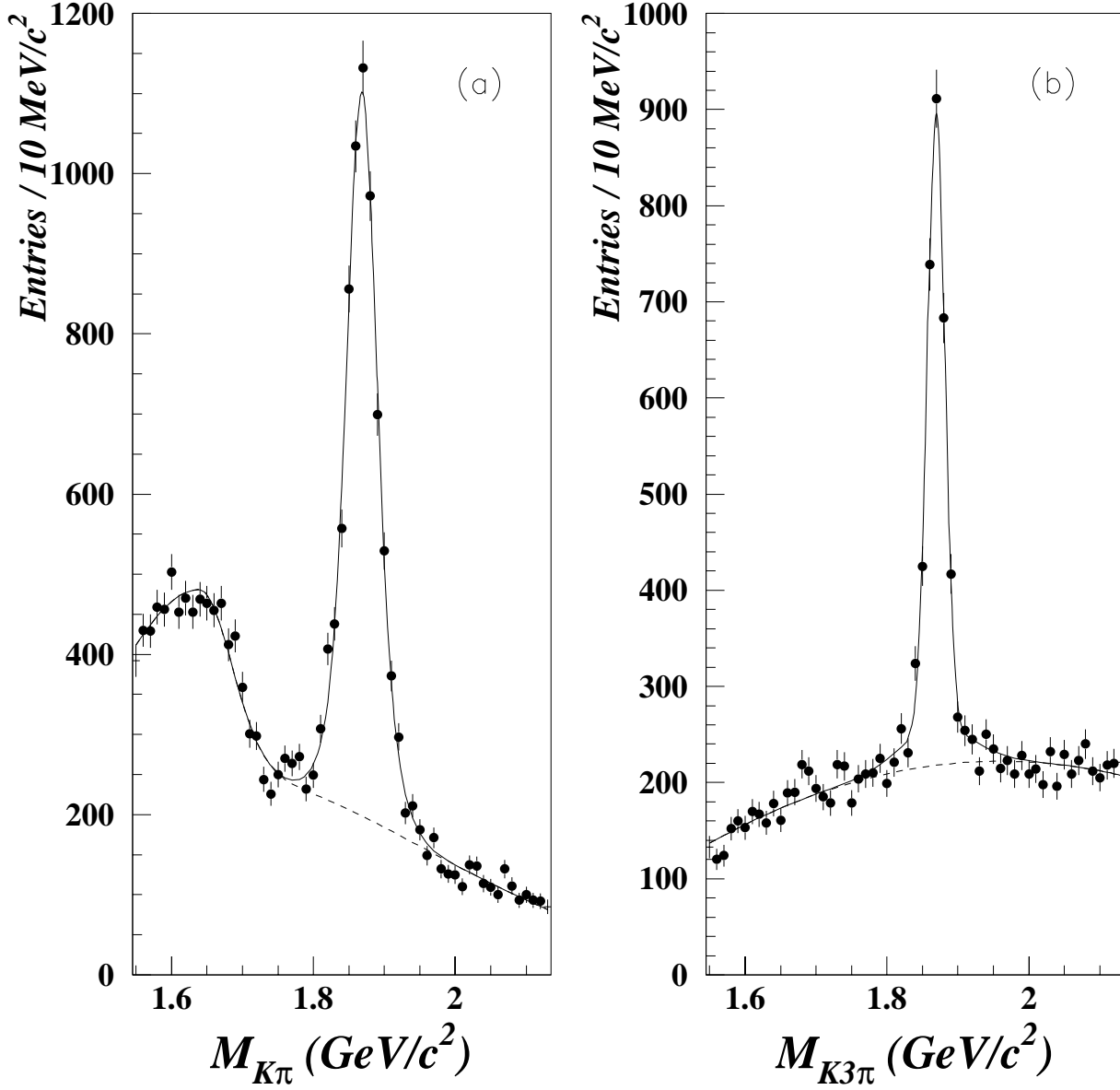


Figure 2: $K\pi$ and $K3\pi$ invariant mass distributions in (a) the $D^{*+} \rightarrow (K^- \pi^+) \pi_{*}^+$ and (b) the $D^{*+} \rightarrow (K^- \pi^+ \pi^+ \pi^-) \pi_{*}^+$ decay channels. The full curve is a fit which includes a background parameterization (dashed curve alone) and two Gaussian functions (see section 4).

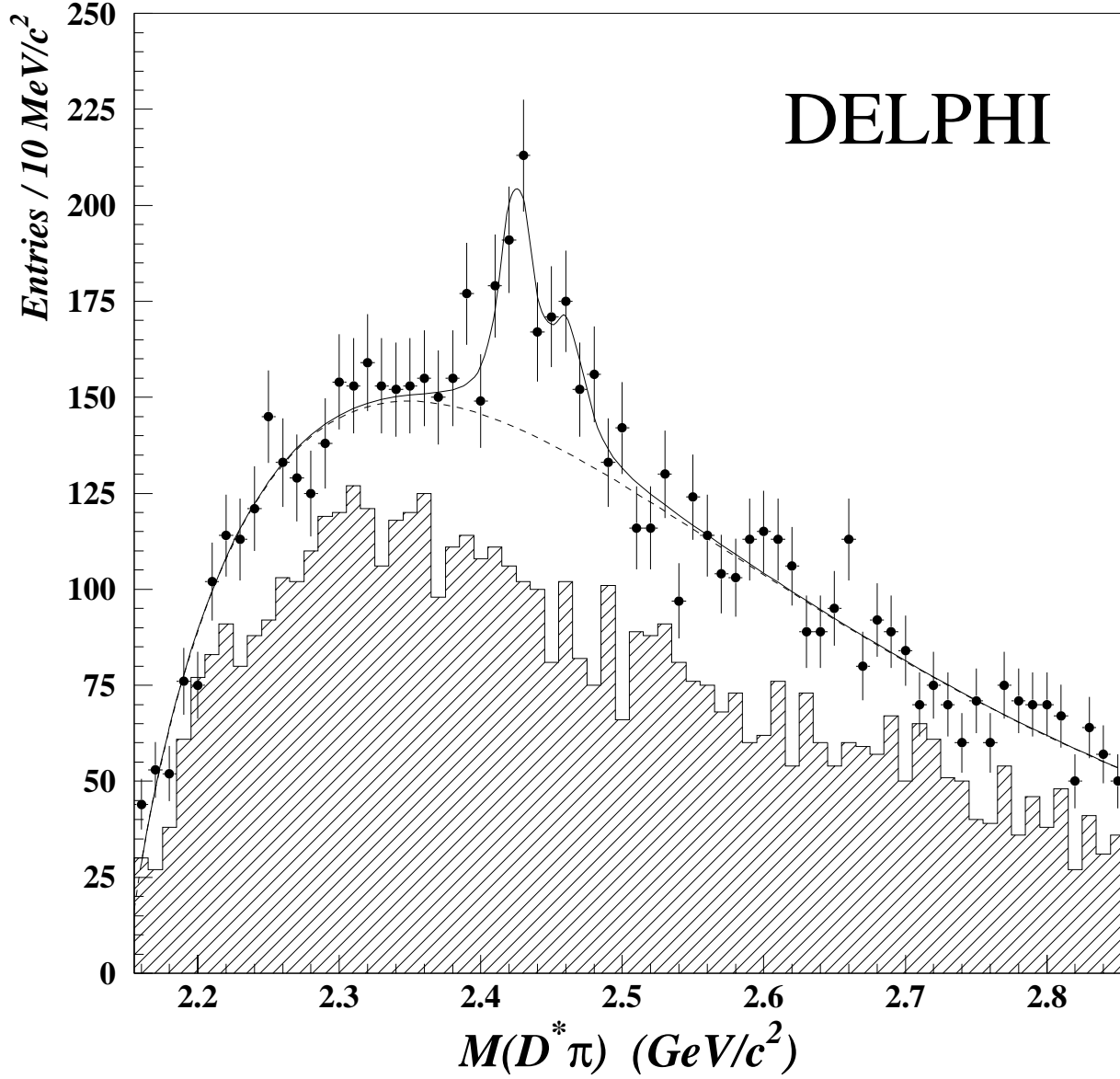


Figure 3: Invariant mass distributions ($D^{*+} \pi^-$) (dots) and ($D^{*+} \pi^+$) (hatched histogram). The mass computation is explained in the text. The full curve is a fit which includes a background parameterization (dashed curve alone) and two Breit-Wigner functions (see section 5).

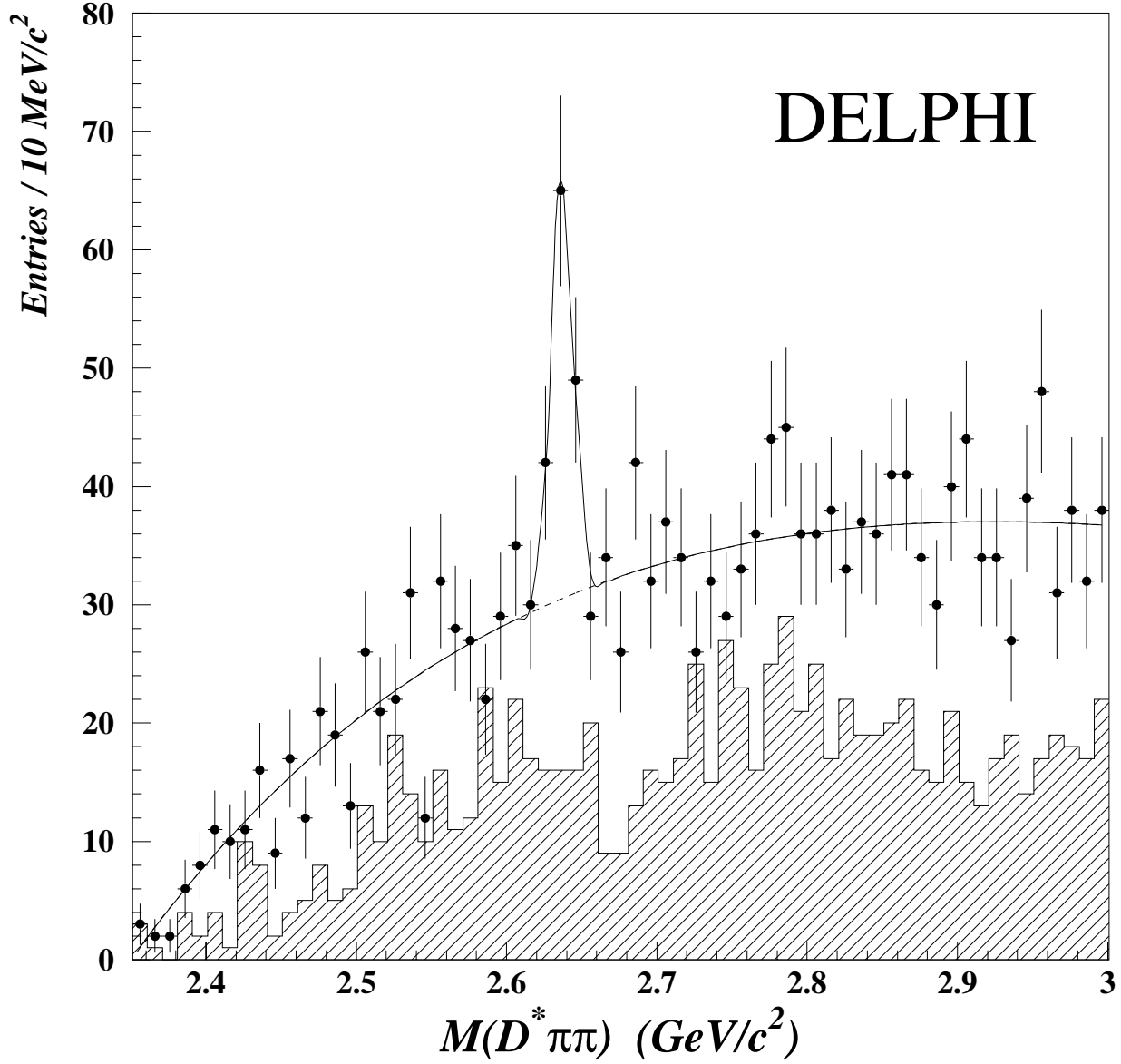


Figure 4: Invariant mass distributions ($D^{*+} \pi^+ \pi^-$) (dots) and ($D^{*+} \pi^- \pi^-$) (hatched histogram). The mass computation is explained in the text. The full curve is a fit which includes a background parameterization (dashed curve alone) and a Gaussian function (see section 6).